Int. J. Heat Mass Transfer. Vol. 21, pp. 407–414. Pergamon Press 1978. Printed in Great Britain

THE BUOYANCY AND VARIABLE VISCOSITY EFFECTS ON A WATER LAMINAR BOUNDARY LAYER ALONG A HEATED LONGITUDINAL HORIZONTAL CYLINDER

LUN-SHIN YAO
The Rand Corporation, Santa Monica, CA 90406, U.S.A.

and

IVAN CATTON
University of California, Los Angeles, CA 90024, U.S.A.

(*Received* 8 *March* 1977 *and in revised form* 26 *July* 1977)

Abstract—The solution of a three-dimensional water boundary layer along a heated horizontal longitudinal hollow cylinder is given. Since the thickness of the boundary layer in the region distance $O(a)$ from the leading edge is thin compared with the radius of the cylinder, the terms of transverse curvature effect can be neglected and the solution is valid for both outer and inner flow provided the induced pressure gradient of inner flow is being neglected. The effects of water variable viscosity on the heat transfer and shear stress distribution are discussed. It has been found that the variable viscosity effect can enhance the heat-transfer rate and can stabilize the boundary-layer flow. On the other hand, the secondary boundary layer induced by the buoyancy forces degrades the heat transfer and destabilizes the boundary layer over the top half of the cylinder.

NOMENCLATURE

a, radius of the cylinder;
b, c, constants, equation (5);
f, nondimensional stream function, equations (9), (10) and (11);
F, similarity nondimensional stream function, equations (14) and (15);
g, similarity nondimensional temperature, equations (10) and (11);
$\bar{g}$, gravitational acceleration, equation (2) = 32.2 ft s^{-2};
G, similarity nondimensional temperature independent of ϕ, equations (14) and (15);
Gr, Grashof number, equation (2);
n, index, equation (17);
N, N_0, N_1, viscosity ratios, equations (2) and (6);
Nu, Nusselt number, equation (21);
Pr, Prandtl number, equation (2);
r, nondimensional coordinate normal to the wall;
$\bar{r}$, radial coordinate;
Re, Reynolds number, equation (2);
T, temperature;
u, axial velocity;
v, circumferential velocity;
w, radial velocity;
x, axial coordinate.

Greek symbols

α, coefficient for variable viscosity;
β, thermal expansion coefficient = 0.8×10^{-4} [°F]$^{-1}$;
$\tilde{\beta}$, coefficient in wedge flow, Fig. 6;
γ, thermal diffusivity;
ε, $= Gr/Re^2$, equation (2);
η, $= r/\sqrt{2x}$, Blasius similarity variable, equation (9);
θ, nondimensional temperature, equation (2);
ν, kinematic viscosity;
ϕ, circumferential coordinate;
τ_{rx}, x-directional shear stress;
$\tau_{r\phi}$, circumferential shear stress.

Subscripts

0, zeroth-order solution;
00, zeroth order of zeroth-order solution;
01, first order of zeroth-order solution;
1, first-order solution;
10, zeroth order of first-order solution;
11, first order of first-order solution;
2, first order cross-flow solution;
w, surface;
∞, free stream;
fc, forced convection.

Superscripts

$\bar{}$, dimensional quantities;
$'$, derivative with respect to η;
x, local quantities at location x.

1. INTRODUCTION

LAMINAR flow control, as the means to achieve low-drag performance, requires the careful manipulation of boundary-layer velocity profiles. Body shaping, pressure gradient, and suction are classic methods for such boundary-layer control [1]. For submersible applications the temperature-dependent viscosity of water provides the mechanism by which appropriate velocity profiles can be maintained by wall heating.

These velocity profiles, as in the other methods, inhibit the amplification of two-dimensional Tollmein–Schlichting instability waves and thus retard boundary-layer transition until body shape and adverse pressure gradient force the separation of the laminar boundary layer. Suction and heating have similar effects on boundary-layer stability and transition, but the theoretical potential of suction for even further drag reduction by delaying laminar separation is greater [2].

Historically, each method of boundary-layer control has had limitations, corresponding to the growth of disturbances associated with free-stream turbulence, surface roughness or waviness, noise, loss of suction effectiveness, or three-dimensionality. Surface heating shares these possible limits on performance and has some limits which are unique to it alone.

Temperature gradients in the boundary layer of a heated horizontal body result in buoyancy forces that induce small, steady, cross-flow velocities. These in turn distort the basic laminar axisymmetric velocity profiles into three-dimensional ones, which are less stable. Yao and Catton [3] earlier examined the development of this steady, slightly three-dimensional laminar boundary layer on a heated longitudinal horizontal cylinder for the case of constant fluid properties. Their results indicate that the buoyancy can enhance the heat transfer and stabilize the boundary layer over the lower half of the cylinder, but it degrades heat transfer and destabilizes the flow over the upper half of the cylinder. Since the boundary layer is very thin compared with the curvature of the cylinder, the transverse curvature effect can be neglected. Also, the results can be applied to the entrance flow in a circular pipe.

The present paper extends that work to the realistic case of water, including the variable viscosity effect. Similarly, the results can be applied to the pipe flow near the entrance. In this way the domain where buoyancy effects may counterbalance the stabilizing variable viscosity effect may be established later.

The physical model chosen is a semi-infinite cylinder of radius a (or in a horizontal pipe with radius a), which is aligned with its axis parallel to a uniform flow and normal to the direction of gravity. The uniform flow is assumed to have a velocity u_∞ and temperature T_∞. The surface of the cylinder is heated to a constant temperature $T_w (T_w > T_\infty)$. For water flow in the range of 40°F (4.4°C) and 100°F (37.8°C), the principal departure from constant property flow is due to viscosity variation. The thermal conductivity and specific heat do not vary appreciably in this range, and the most important phenomena, because of the gradient of viscosity, are quite well represented by the model in which k and c_p are constant, and the variation of viscosity with temperature is preserved. Since the density variation is small, the Boussinesq approximation is adopted, which treats the density as a constant in the equations of motion except for the buoyancy force term. The buoyancy cross flow is small in the region distance $O(a)$ from the leading edge of the cylinder and can be treated as a second-order effect. Further downstream, a distance of order $a \cdot Re/Gr^{1/2}$, the initially small buoyancy cross flow becomes one of the dominant velocity components and can no longer be treated as a second-order effect. For example, the analysis should provide an accurate approximation to the buoyancy effect in the region $0 < \bar{x} < a/\sqrt{\varepsilon} = (u_\infty/\sqrt{(\beta \bar{g} \Delta T)} \cdot \sqrt{a})$.

The ratio of the cross-flow component to the free-stream velocity is $\beta g \Delta T \bar{x}/u_\infty^2 \sin\phi$.

2. ANALYSIS

The governing equations of the flow with fluid of variable viscosity on a heated, longitudinal, horizontal cylinder are the Boussinesq boundary-layer equations. In cylindrical coordinates, as shown in Fig. 1, they are

$$\frac{\partial \bar{u}}{\partial \bar{x}} + \frac{1}{\bar{r}} \frac{\partial (\bar{r}\bar{w})}{\partial \bar{r}} + \frac{1}{\bar{r}} \frac{\partial \bar{v}}{\partial \phi} = 0 \tag{1a}$$

$$\bar{u} \frac{\partial \bar{u}}{\partial \bar{x}} + \frac{\bar{v}}{\bar{r}} \frac{\partial \bar{u}}{\partial \phi} + \bar{w} \frac{\partial \bar{u}}{\partial \bar{r}} = \frac{-1}{\rho_\infty} \frac{\partial \bar{p}}{\partial \bar{x}} + \frac{\partial}{\partial \bar{r}} \left(\nu \frac{\partial \bar{u}}{\partial \bar{r}} \right) \tag{1b}$$

$$\bar{u} \frac{\partial \bar{w}}{\partial \bar{x}} + \frac{\bar{v}}{\bar{r}} \frac{\partial \bar{w}}{\partial \phi} + \bar{w} \frac{\partial \bar{w}}{\partial \bar{r}} = (\bar{g}\beta \Delta T) \cos\phi - \frac{1}{\rho_\infty} \frac{\partial \bar{p}}{\partial \bar{r}} + \frac{\partial}{\partial \bar{r}} \left(\nu \frac{\partial \bar{w}}{\partial \bar{r}} \right) \tag{1c}$$

$$\bar{u} \frac{\partial \bar{v}}{\partial \bar{x}} + \frac{\bar{v}}{\bar{r}} \frac{\partial \bar{v}}{\partial \phi} + \bar{w} \frac{\partial \bar{v}}{\partial \bar{r}} = (\bar{g}\beta \Delta T) \sin\phi - \frac{1}{\bar{r}\rho_\infty} \frac{\partial \bar{p}}{\partial \phi} + \frac{\partial}{\partial \bar{r}} \left(\nu \frac{\partial \bar{v}}{\partial \bar{r}} \right) \tag{1d}$$

$$\bar{u} \frac{\partial T}{\partial \bar{x}} + \frac{\bar{v}}{\bar{r}} \frac{\partial T}{\partial \phi} + \bar{w} \frac{\partial T}{\partial \bar{r}} = \alpha \frac{\partial^2 T}{\partial \bar{r}^2}. \tag{1e}$$

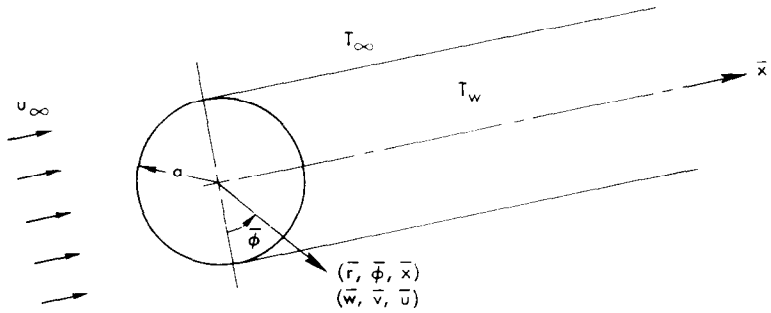

FIG. 1. Physical model and coordinates.

Equations (1) are also valid for the entrance flow in a heated pipe.

The dimensionless variables that are introduced to nondimensionalize equations (1) are

$$\left.\begin{aligned} &u=\frac{\bar{u}}{u_\infty},\quad v=\frac{\bar{v}}{u_\infty},\quad w=\frac{\bar{w}\sqrt{Re}}{u_\infty} && \text{(the velocities)}\\ &\theta=\frac{T-T_\infty}{T_w-T_\infty} && \text{(the temperature)}\\ &x=\frac{\bar{x}}{a},\quad r=\frac{(\bar{r}-a)\sqrt{Re}}{a} && \text{(the coordinates)}\\ &Re=\frac{u_\infty a}{\nu} && \text{(the Reynolds number)}\\ &Gr=\frac{\beta\bar{g}a^3(T_w-T_\infty)}{\nu^2} && \text{(the Grashof number)}\\ &Pr=\frac{\nu_\infty}{\gamma} && \text{(the Prandtl number)}\\ &\varepsilon=\frac{Gr}{Re^2}\\ &N=\frac{\mu}{\mu_\infty}. \end{aligned}\right\}\quad (2)$$

The radius of the cylinder, a, has been selected as the longitudinal characteristic length in order to study the detailed development of the mechanism of the induced cross flow caused by heating along the upstream part of the horizontal cylinder. The coordinate normal to the wall has been stretched to reflect the fact that the thickness of the boundary layer in the region of $\bar{x} \sim O(a)$ is inversely proportional to the square root of the Reynolds number.

We note that the quantity ε can be expressed simply as $\beta g(T_w-T_\infty)a/u_\infty^2$ and can be interpreted as the ratio of the potential energy increment to the kinetic energy of the flow. For the flow close to the leading edge of the cylinder (or close to the entrance of a pipe), the magnitude of ε determines the importance of the thermally driven cross flow. As we move further downstream, the governing parameter will be the Grashof number instead of ε. There the buoyancy can be neglected only when the Grashof number is small. For our case, where the Grashof number is not small but Gr/Re^2 is small, the buoyancy effect can be treated as a secondary effect in the region near the leading edge of the cylinder (or near the entrance of the pipe). The magnitude of the cross flow develops and eventually becomes important which can trigger the flow transition and the flow separation further downstream. It is worth noting that the value of ε also determines the size of the early region where the cross flow is a second-order effect when $Gr > 1$ and $Gr/Re^2 < 1$. In terms of the dimensionless parameters in equation (2), equations (1) become

$$\frac{\partial u}{\partial x}+\frac{\partial w}{\partial r}+\frac{\partial v}{\partial \phi}=0 \quad (3a)$$

$$u\frac{\partial u}{\partial x}+v\frac{\partial u}{\partial \phi}+w\frac{\partial u}{\partial r}=-\frac{\partial p}{\partial x}+\frac{\partial}{\partial r}\left(N\frac{\partial u}{\partial r}\right) \quad (3b)$$

$$\frac{\partial p}{\partial r}=\frac{\varepsilon}{\sqrt{Re}}\cdot\theta\cdot\cos\phi \quad (3c)$$

$$u\frac{\partial v}{\partial x}+v\frac{\partial v}{\partial \phi}+w\frac{\partial v}{\partial r}=\varepsilon\cdot\sin\phi\cdot\theta-\frac{\partial p}{\partial \phi}+\frac{\partial}{\partial r}\left(N\frac{\partial v}{\partial r}\right) \quad (3d)$$

$$u\frac{\partial \theta}{\partial x}+v\frac{\partial \theta}{\partial \phi}+w\frac{\partial \theta}{\partial r}=\frac{1}{Pr}\frac{\partial^2\theta}{\partial r^2} \quad (3e)$$

after neglecting smaller-order terms. The terms that represent the transverse curvature effect have been neglected simply because the boundary layer is thin compared with the radius of the cylinder when the Reynolds number is not small. Equation (3c) indicates that the pressure gradient normal to the wall is negligible to the lowest order, and the pressure gradients parallel to the wall can be evaluated from the inviscid solution at the edge of the boundary layer. For a uniform free stream, these pressure gradients vanish.

It is necessary to specify the viscosity ratio, N, before the solutions of equations (3) can be presented. It has been shown by Gazley* that a good approximation for the kinematic viscosity of water in the range of temperature between 4.4 and 37.8°C is

$$\nu=\frac{10^{-4}}{0.3471+0.0244T} \quad (4)$$

where T is in °C and ν is in $m^2 s^{-1}$. This suggests a viscosity–temperature model of the form

$$\mu=\frac{1}{b+cT}. \quad (5)$$

For such a model,

$$\frac{1}{N}=\frac{\mu_\infty}{\mu}=1+\alpha\Delta T\cdot\theta \quad (6)$$

where $\Delta T = T_w - T_\infty$, and $\alpha = c/(b+cT_\infty)$. For water in the temperature range between 4.4 and 37.8°C, $\alpha \approx 0.0272\ (°C)^{-1}$. It has also been shown by Gazley that the Prandtl number of water in the range of temperature 4.4 and 37.8°C can be approximated by

$$Pr=\frac{455}{32+1.8T_\infty} \quad (7)$$

where T_∞ is in °C. The illustrative calculations described below were performed using a value of $Pr = 8$.

The solution of equation (3) with the viscosity–temperature model, equation (6), can be expanded into a series in ε, if ε is small, so that

$$u=u_0+\varepsilon u_1+\ldots \quad (8a)$$

$$v=\varepsilon v_1+\ldots \quad (8b)$$

$$w=w_0+\varepsilon w_1+\ldots \quad (8c)$$

$$\theta=\theta_0+\varepsilon\theta_1+\ldots \quad (8d)$$

$$N=N_0+\varepsilon N_1+\ldots \quad (8e)$$

*Personal communication from Carl Gazley, Jr., The Rand Corporation, 1976.

where

$$N_0 = \frac{1}{1+\alpha\Delta T\,\theta_0} \tag{8f}$$

$$N_1 = \frac{-\alpha\Delta T}{(1+\alpha\Delta T\,\theta_0)^2}\cdot\theta_1 = -A(\theta_0)\cdot\theta_1. \tag{8g}$$

Substitution of the expansion given by equations (8) into equations (3), and the collection of terms of equal order will result in the perturbation equations. The perturbation equations of lowest order are

$$(\varepsilon^0): \quad (N_0 f_0'')' + f_0 f_0'' = 0 \tag{9a}$$

$$\theta_0'' + Pr\, f_0\theta_0' = 0 \tag{9b}$$

where the prime denotes a derivative with respect to η, with $\eta = r/\sqrt{2x}$ being the Blasius similarity variable. The stream function f_0 is defined by

$$u_0 = f_0' \tag{9c}$$

$$w_0 = \frac{1}{\sqrt{2x}}(\eta f_0' - f_0). \tag{9d}$$

The second-order perturbation equations are

$$(\varepsilon^1): \quad (N_0 f_1'')' + f_0 f_1'' - 4f_0' f_1' + 5f_0'' f_1 + f_0''\frac{\partial f_2}{\partial\phi} = (A\cdot g\cdot f_0'')' \tag{10a}$$

$$(N_0 f_2'')' + f_0 f_2'' - 2f_0' f_2' + \sin\phi\cdot\theta_0 = 0 \tag{10b}$$

$$\frac{1}{Pr}g'' + f_0 g' - 4f_0' g + 5\theta_0' f_1 + \theta_0'\frac{\partial f_2}{\partial\phi} = 0. \tag{10c}$$

The stream functions f_1 and f_2 and the temperature g are defined by

$$\left.\begin{aligned} u_1 &= (2x)^2 f_1'(\eta,\phi)\\ v_1 &= (2x) f_2'(\eta,\phi)\\ w_1 &= (2x)^{3/2}\left(\eta f_1' - 5f_1 - \frac{\partial f_2}{\partial\phi}\right)\\ \theta_1 &= (2x)^2 g(\eta,\phi). \end{aligned}\right\} \tag{11}$$

The boundary conditions associated with equations (9) are

$$\left.\begin{aligned} f_0 = f_0' = 0 \quad &\text{and} \quad \theta_0 = 1 \quad \text{at} \quad \eta = 0\\ f_0' \to 1 \quad &\text{and} \quad \theta_0 \to 0 \quad \text{as} \quad \eta \to \infty \end{aligned}\right\} \tag{12}$$

and the ones associated with equations (10) are

$$\left.\begin{aligned} f_1' = f_2' = f_1 = \frac{\partial f_2}{\partial\phi} = 0, \quad & g = 0 \text{ at } \eta = 0\\ f_1' = f_2' = 0, \quad & g = 0 \text{ as } \eta \to \infty\\ f_2' = 0 \quad & \text{at } \phi = 0, \pi. \end{aligned}\right\} \tag{13}$$

Equations (10) are separable in terms of η and ϕ with dependent variables of the form

$$\left.\begin{aligned} f_1(\eta,\phi) &= F_1(\eta)\cos\phi\\ f_2(\eta,\phi) &= F_2(\eta)\sin\phi\\ g(\eta,\phi) &= G(\eta)\cos\phi. \end{aligned}\right\} \tag{14}$$

Substituting equations (14) into equations (10) gives

$$(N_0 F_1'')' + f_0 F_1'' - 4f_0' F_1' + 5f_0'' F_1 + f_0'' F_2 = (A\cdot G\cdot f_0'')' \tag{15a}$$

$$(N_0 F_2'')' + f_0 F_2'' - 2f_0' F_2' = -\theta_0 \tag{15b}$$

$$\frac{1}{Pr}G'' + f_0 G' - 4f_0' G = -\theta_0'(5F_1 + F_2) \tag{15c}$$

The associated boundary conditions for equations (10) are

$$\left.\begin{aligned} F_1(0) = F_1'(0) = F_1'(\infty) = 0\\ F_2(0) = F_2'(0) = F_2'(\infty) = 0\\ G(0) = G(\infty) = 0 \end{aligned}\right\} \tag{16}$$

The solutions depend on temperature only through the factor $\alpha\Delta T$ and are integrated numerically for $\alpha\cdot\Delta T = 0, 0.5, 1.0$. If $T_\infty = 13^\circ$C, this corresponds to $\Delta T = 0$, 18.3°, 36.7°.

3. NUMERICAL RESULTS

The physical quantities of velocity and temperature can be expressed in terms of the functions defined in equations (8), (9) and (11). They are:

$$u = f_0' + \varepsilon(2x)^2 F_1'\cdot\cos\phi + \ldots \tag{17a}$$

$$v = \varepsilon(2x)\cdot F_2'\cdot\sin\phi + \ldots \tag{17b}$$

$$w = \frac{1}{(2x)^{1/2}}(\eta f_0' - f_0) + \varepsilon(2x)^{3/2}(\eta F_1' - 5F_1 - F_2)\cdot\cos\phi + \ldots \tag{17c}$$

$$\theta = \theta_0 + \varepsilon(2x)^2\cdot G\cdot\cos\phi + \ldots. \tag{17d}$$

The local shear stress at the cylinder can be computed from the axial and cross-flow velocity components:

$$\tau_{rx} = \mu\left(\frac{\partial\bar{u}}{\partial\bar{r}}\right)_{r=0} \quad \text{and} \quad \tau_{r\phi} = \mu\left(\frac{\partial\bar{v}}{\partial r}\right)_{r=0}$$

Introducing the series expansion (17), this can be written as

$$\frac{\tau_{rx}}{(\tau_{rx})_{fc}} = 1 + \varepsilon(2x)^2\frac{F_1''(0)}{f_0''(0)}\cdot\cos\phi + \ldots \tag{18}$$

for the axial shear and

$$\frac{\tau_{r\phi}}{(\tau_{rx})_{fc}} = \varepsilon\cdot(2x)^{1/2}\cdot\frac{F_2''(0)}{f_0''(0)}\cdot\sin\phi \tag{19}$$

for the circumferential component, where fc denotes the value for forced convection with variable viscosity.

The local Nusselt number can be written as

$$\frac{Nu}{Nu_{fc}} = 1 + \varepsilon(2x)^2\cdot\frac{G'(0)}{\theta_0'(0)}\cdot\cos\phi + \ldots. \tag{20}$$

Table 1 shows the values of the quantities $F_1''(0)/f_0''(0)$, $G'(0)/\theta_0'(0)$, and $F_2''(0)$.

Table 1. Enhancement parameters for heat transfer and wall shear stress

	$G'(0)/\theta_0'(0)$	$F_1''(0)/f_0''(0)$	$F_2''(0)/f_0''(0)$
$\alpha = 0$	0.06981	0.04905	0.88385
$\alpha\Delta T = 0.5$	0.06559	0.04897	0.80439
$\alpha\Delta T = 1.0$	0.06296	0.04899	0.75967

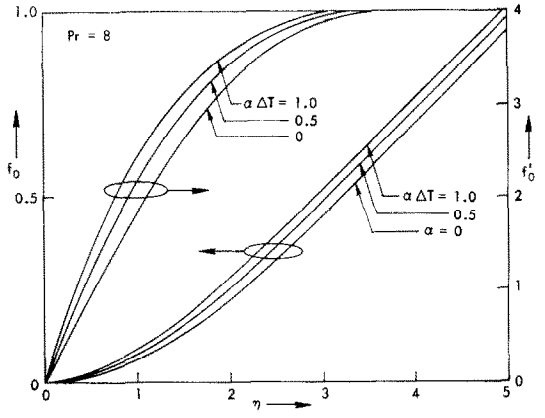

FIG. 2. Stream function and velocity profiles without cross flow.

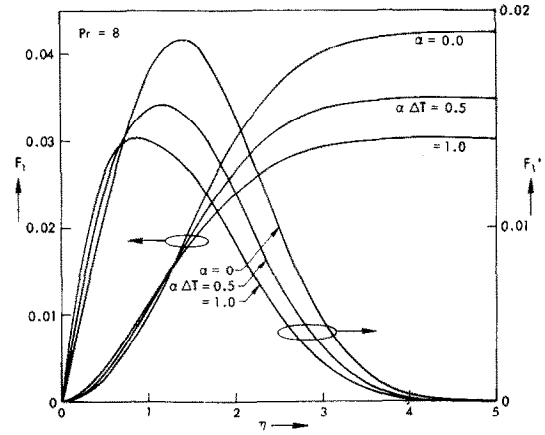

FIG. 3. F_1 and F_1' functions.

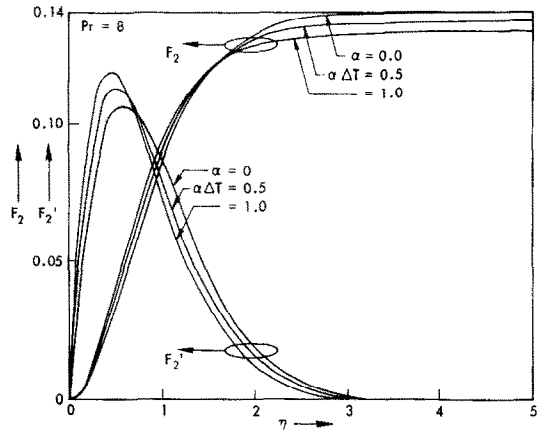

FIG. 4. F_2 and F_2' functions.

From Figs. 2–4 we observe that the reduction of water viscosity caused by heating modifies the axial flow: The axial flow is accelerated by the induced cross flow over the lower half of the cylinder ($-\pi/2 < \phi < \pi/2$) and decelerated over the upper half ($\pi/2 < \phi < 3\pi/2$). The cross flow is accelerated by buoyancy from the lower stagnation point ($\phi = 0$) to its maximum value at $\phi = \pi/2$ and then decelerated to its upper stagnation point ($\phi = \pi$). The decrease of viscosity by heating enhances the magnitude of the cross flow (F_2') and shifts the point of maximum velocity toward the wall as shown in Fig. 4. Therefore, the cross-flow velocity gradient at the wall is magnified appreciably by a slight variation of the fluid viscosity. The induced axial velocity profile F_1' becomes fuller in the wall region, as wall temperature increases. The key differences between the cross-flow velocity F_2' and the co-induced axial velocity F_1' is that the maximum value of F_2' increases from 0.118 to 0.107 as $\alpha\Delta T$ increases from 0 to 1, while the maximum value of F_1' decreases from 0.021 to 0.015 over the same range.

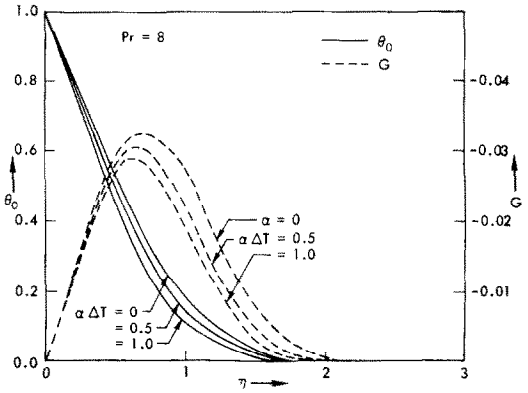

FIG. 5. Temperature distribution.

From Fig. 5 it can be seen that the effect of heating on the buoyancy correction G is negligible in the region near the wall, but the maximum value of G decreases slightly as $\alpha\Delta T$ increases. Since the maximum value of G is only 0.03, the cross-flow effect on the temperature field is negligible in this region. However, the primary distribution of the temperature gradient, θ_0', varies about 10% in the range between $\alpha = 0$ and $\alpha\Delta T = 1$.

4. BUOYANCY VERSUS VARIABLE VISCOSITY

The primary importance of cross flow is the stability of the resulting three-dimensional boundary layer, and this will be considered in subsequent research. However, it is still of some interest to compare the magnitudes of the buoyancy effect with the variable viscosity effect, in order to further delineate the region where buoyancy effects on shear stress, heat transfer and separation may safely be neglected.

While the solutions of equations (9) and (15) correspond to the most general case of arbitrarily large viscosity variation, explicit estimates of the region where buoyancy effects on heat transfer and axial velocity profiles start to be important can be obtained by a further approximation.

If the viscosity variation is small, because of small values of $\alpha\Delta T$, the effect of variable viscosity can be separated out from the first-order equations (9a) and (9b) by a linearization procedure. When $\alpha = 0$, the solution of equation (9a) corresponds to the Blasius solution. The expansion procedure becomes

$$\left.\begin{aligned} f_0 &= f_{00} + (\alpha\Delta T)\cdot f_{01} + \dots \\ \theta_0 &= \theta_{00} + (\alpha\Delta T)\cdot\theta_{01} + \dots \end{aligned}\right\}. \tag{21}$$

heating will increase the axial velocity gradient on the wall and consequently will tend to stabilize the boundary layer [2, 3]. For a horizontal cylinder, the cross flow will be induced by wall heating as a by-product, which will decrease the axial velocity gradient on the wall. In general, the stability of a boundary layer can be related to this velocity gradient on the wall as has been demonstrated by Wazzan and Gazley, Jr. [4] and shown in Fig. 6. Based on this observation, the

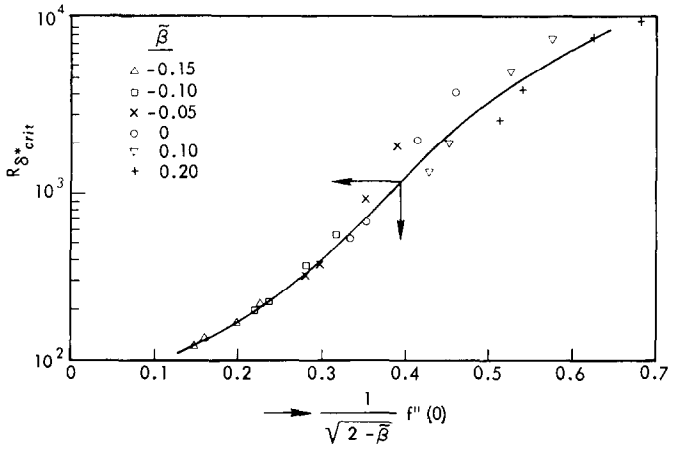

FIG. 6. Critical Reynolds number vs wall velocity gradient.

Substitution of equations (17) into equations (9a) and (9b), or collecting terms of equal order, gives the equations of the zeroth order

$$f_{00}''' + f_{00}f_{00}'' = 0 \tag{22a}$$

$$\frac{1}{Pr}\theta_{00}'' + f_{00}\theta_{00}' = 0 \tag{22b}$$

and the equations of the first order

$$f_{01}''' + (f_{00}f_{01}'' + f_{00}''f_{01}) = (\theta_{00}f_{00}'')' \tag{23a}$$

$$\frac{1}{Pr}\theta_{01}'' + f_{00}\theta_{01}' + f_{01}\theta_{00}' = 0. \tag{23b}$$

The associated boundary conditions

$$\left.\begin{aligned} &f_{00}(0) = f_{00}'(0) = 0, && f_{00}'(\infty) = 1 \\ &\theta_{00}(0) = 1, && \theta_{00}(\infty) = 0 \\ &f_{01}(0) = f_{01}'(0) = f_{01}'(\infty) = 0 \\ &\theta_{01}(0) = \theta_{01}(\infty) = 0. \end{aligned}\right\} \tag{24}$$

The solution of equation (22a) is the Blasius solution; the solution of equation (22b) is the forced-convection energy equation. The functions f_{01} and θ_{01} represent the effect of the variable viscosity on the forced convection. The numerical values of θ_{01} and f_{01} can be obtained by integrating equation (23) numerically. Strictly speaking, the above approach is valid only for small values of $\alpha\Delta T$. However, comparison with the solution of equation (9) shows that this linearization is accurate in the range $0 < \alpha\Delta T < 0.5$.

The decrease of the water viscosity caused by cross flow seems to introduce a destabilizing effect on the boundary layer. Also, the inflection point of the cross-flow velocity profile could be unstable. The conditions leading to flow transition can only be defined by extensive stability analysis. Before we can exercise such a complicated three-dimensional stability analysis, we will apply a simple criterion, the variation of axial velocity grdient on the wall, to study the tendency of stabilizing or destabilizing the boundary layer by heating.

The purpose of the study in this section is to provide some insight into the balancing effects of variable viscosity and cross flow. Thus the discussion is limited to the case of small values of $\alpha\Delta T$ in order to supply a simple criterion to define a region and its functional dependence that heating is a practical way to stabilize the boundary layer.

The double expansion of velocity and temperature in terms of ε and $\alpha\Delta T$ can be written:

$$u = f_{00}' + (\alpha\Delta T)f_{01}' + \varepsilon(2x)^2[F_{10}' + (\alpha\Delta T)F_{11}']\cos\phi + \dots \tag{25a}$$

$$\theta = \theta_{00} + (\alpha\Delta T)\theta_{01} + \varepsilon(2x)^2[G_0 + (\alpha\Delta T)G_1]\cos\phi + \dots \tag{25b}$$

where

$$\left.\begin{aligned} F_1 &= F_{10} + (\alpha\Delta T)F_{11} + \dots \\ G &= G_0 + (\alpha\Delta T)G_1 + \dots \end{aligned}\right\} \tag{26}$$

and F_{10} and G_0 are the first-order-solution, cross-flow-induced quantities, with a constant property assumption. The equations governing F_{10} and G_0 are equations (15) with $N_0 = 1$ and $A = 0$.

The local shear stress, equation (18), can be further expanded. It becomes

$$\frac{\tau_{rx}}{(\tau_{rx})_{fc}} = 1+(\alpha\Delta T)\frac{f''_{01}(0)}{f''_{00}(0)} + \varepsilon(2x)^2\frac{F''_{10}}{f''_{00}(0)}\cdot\cos\phi+\ldots \quad (27)$$

where fc denotes the case of forced convection with constant viscosity. Since the wall viscosities are the same, equation (27) can be viewed as the ratio of the velocity gradients at the wall. Values of $f''_{01}(0)/f''_{00}(0)$ and $F''_{10}(0)/f''_{00}(0)$ are given in Table 2, and $f''_{01}(0)/f''_{00}(0)$ is about twenty times bigger than $F''_{10}(0)/f''_{00}(0)$. This

Table 2. Ratios of heat flux and shear stress

$f''_{01}(0)/f''_{00}(0)$	$F''_{10}(0)/f''_{00}(0)$	$\theta'_{01}(0)/\theta'_{00}(0)$	$G'_0(0)/\theta'_{00}(0)$
0.89169	0.04905	0.17791	0.06981

indicates that the variable viscosity effect overwhelms the buoyancy effect over the most forward part of the cylinder. However, the magnitude of the cross-flow effect increases as $\sim x^2$ downstream. The variable-viscosity effect is eventually balanced by the buoyancy effect far away from the leading edge. Equation (27) clearly points out the location where the effect of stabilizing the boundary layer by heating will be balanced by the destabilizing buoyancy effect over the upper half of the cylinder ($\pi/2 < \phi < 3\pi/2$). This location can be found from equation (27) by equating the second and the third terms on the RHS, which yields

$$x = \tfrac{1}{2}\left[\frac{(\alpha\Delta T)}{\varepsilon}\frac{f''_{01}(0)}{F''_{10}(0)}\right]^{1/2}\cdot\frac{1}{(|\cos\phi|)^{1/2}}. \quad (28)$$

Equation (28) is plotted in Fig. 7, which shows that the region of stabilizing the boundary layer by heating shrinks as x increases. It should be noted that the expansions (22) are valid only up to $x \sim O(1/\sqrt{\varepsilon})$ and then the originally small cross flow becomes one of the dominant velocity components beyond $x \sim O(1/\sqrt{\varepsilon})$ when Gr is not small. Equation (28), however, indicates that the merit of the heating to stabilize the boundary layer starts to fade away at $x \sim O(\alpha\Delta T/\varepsilon)^{1/2}$ and disappears before the magnitude of the cross flow becomes appreciable, if $\alpha\Delta T$ is small.

Similarly, the relative importance of heat transfer due to buoyancy and variable viscosity can be obtained by further expanding equation (21)

$$\frac{Nu_x}{(Nu_x)_{fc}} = 1+(\alpha\Delta T)\frac{\theta'_{01}(0)}{\theta'_{00}(0)} + \varepsilon(2x)^2\cdot\frac{G'_0(0)}{\theta'_{00}(0)}\cdot\cos\phi+\ldots \quad (29)$$

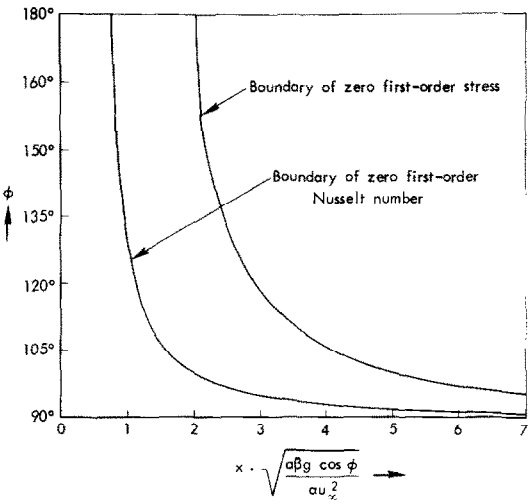

FIG. 7. Boundary where the variable viscosity effect balances the cross flow-effect.

if $(\alpha\Delta T)$ is small. Values of $\theta'_{01}(0)/\theta'_{00}(0)$ and $G'_0(0)/\theta'_{00}(0)$ are listed in Table 2. Equation (29) shows that the cross flow enhances the heat transfer on the lower half of the cylinder and degrades it on the upper half of the cylinder. The boundary where the variable viscosity effect is balanced by the buoyancy can be obtained similarly as the way to get equation (28). It is

$$x = \tfrac{1}{2}\left[\frac{(\alpha\Delta T)}{\varepsilon}\frac{\theta'_{01}(0)}{G'_0(0)}\right]^{1/2}\cdot\frac{1}{(|\cos\phi|)^{1/2}} \quad (30)$$

The explicit expression of equations (28) and (30) in terms of physical quantities can be written as

$$x \sim \left(\frac{\alpha}{a\beta g\cos\phi}\right)^{1/2}\cdot u_\infty. \quad (31)$$

Equation (31) reveals that the size of the stabilized region by heating is proportional to the free stream speed, is inversely proportional to the square root of the cylinder diameter, and is independent of ΔT.

REFERENCES

1. H. Schlichting, *Boundary Layer Theory*, 6th edn. McGraw-Hill, New York (1968).
2. J. Aroesty and S. A. Berger, Controlling the separation of laminar boundary layers in water: heating and suction. The Rand Corporation, R-1789-ARPA (September 1975).
3. L. S. Yao and I. Catton, Buoyancy cross-flow effects on the boundary layer of a heated horizontal cylinder, *J. Heat Transfer* **99C**, 122 (1977).
4. A. R. Wazzan and C. Gazley, Jr., A parametric study of boundary-layer stability and transition for Falkner–Skan wedge flows, Presentation at *Low-Speed Boundary-Layer Transition Workshop: II*, held at The Rand Corporation, Santa Monica, California (13–15 September 1976).

LES EFFETS DE LA GRAVITATION ET DE LA VISCOSITE VARIABLE SUR UNE COUCHE LIMITE LAMINAIRE D'EAU LE LONG D'UN CYLINDRE HORIZONTAL ET ET CHAUFFE

Résumé—On donne la solution d'une couche limite tridimensionnelle d'eau le long d'un cylindre creux, horizontal et chaud. Puisque l'épaisseur de la couche limite dans la région de distance $O(a)$ à partir du bord d'attaque est mince en comparaison du rayon du cylindre, les termes de l'effet de courbure transversale peuvent être négligés et la solution est valide à la fois pour les écoulements interne et externe tant que le gradient de pression induit de l'écoulement interne peut être négligé. Les effets de la viscosité variable de l'eau sur le transfert thermique et la tension de frottement sont discutés. On trouve que l'effet de viscosité variable accroit le transfert thermique et peut stabiliser l'écoulement de couche limite. Par contre, la couche limite secondaire induite par les forces de gravité diminue le transfert thermique et déstabilise la couche limite sur la moitié supérieure du cylindre.

DER EINFLUß DES AUFTRIEBS UND DER VARIABLEN VISKOSITÄT AUF EINE LAMINARE WASSER-GRENZSCHICHT LÄNGS EINES BEHEIZTEN HORIZONTALEN ZYLINDERS

Zusammenfassung—Die Lösung für eine dreidimensionale Wasser-Grenzschicht längs eines beheizten horizontalen Hohlzylinders wird angegeben. Da die Dicke der Grenzschicht im Bereich O(a) von der Anströmseite her klein ist bezüglich des Zylinder-Radiusses, kann der Einfluß der Querkrümmung vernachlässigt werden, und die Lösung wird sowohl für die äußere—wie die innere Strömung unter der Voraussetzung gültig, daß der Druckgradient der inneren Strömung vernachlässigt wird. Der Einfluß der veränderlichen Viskosität des Wassers auf den Wärmeübergang und die Schubspannungsverteilung wird diskutiert. Es ergab sich, daß die veränderliche Viskosität den Wärmeübergang verbessern und die Grenzschichtströmung stabilisieren kann. Die Sekundär-Grenzschicht, die durch die Auftriebskräfte hervorgerufen wird, verringert andererseits den Wärmeübergang und destabilisiert die Grenzschicht über der oberen Hälfte des Zylinders.

ВЛИЯНИЕ СВОБОДНОЙ КОНВЕКЦИИ И ПЕРЕМЕННОЙ ВЯЗКОСТИ НА ЛАМИНАРНЫЙ ПОГРАНИЧНЫЙ СЛОЙ ПРИ ПРОДОЛЬНОМ ОБТЕКАНИИ ВОДОЙ НАГРЕТОГО ГОРИЗОНТАЛЬНОГО ЦИЛИНДРА

Аннотация — Приводится решение для трехмерного пограничного слоя при продольном обтекании водой нагретого горизонтального полого цилиндра. Поскольку толщина пограничного слоя в области, отстоящей на расстоянии 0(a) от передней кромки, мала по сравнению с радиусом цилиндра, влиянием членов, учитывающих поперечную кривизну, можно пренебречь, и тогда решение будет справедливым как для внешнего, так и для внутреннего обтекания при условии пренебрежения градиентом давления, возникающем в потоке внутри цилиндра. Рассматривается влияние переменной вязкости воды на интенсивность переноса тепла и распределение касательных напряжений. Показано, что переменная вязкость может интенсифицировать перенос тепла и стабилизировать течение в пограничном слое. С другой стороны, вторичный пограничный слой, возникающий из-за свободноконвективного восходящего движения жидкости, ухудшает теплообмен и вносит возмущения в пограничный слой в верхней части цилиндра.